Springer

KSME

Journal of Mechanical Science and Technology 31 (12) (2017) 5687~5693
www.springerlink.com/content/1738-494x(Print)/1976-3824(Online)
DOI 10.1007/s12206-017-1109-x

Ultrasonic thermoforming of a large thermoplastic polyurethane film with the aid of infrared heating †

Hyun-Joong Lee, Dong-Ju Shin and Keun Park*

Department of Mechanical System Design Engineering, Seoul National University Science and Technology, Seoul 01811, Korea

(Manuscript Received July 13, 2017; Revised August 3, 2017; Accepted August 3, 2017)

Abstract

This study concerns ultrasonic thermoforming of Thermoplastic polyurethane (TPU) film for the fabrication of a television speaker diaphragm. The speaker diaphragm has a convex-protruded feature with a rounded-rectangular shape on which a number of micro-corrugations are formed for sound quality improvement. This diaphragm has generally been manufactured out of thin TPU film using a thermoforming process, which required cycle time as long as several minutes for proper heating and cooling of the polymer film and mold. In this study, an ultrasonic thermoforming process was introduced to reduce the cycle time to fabricate the diaphragm by taking advantage of the rapid and localized heating capability of ultrasonic vibration energy. To improve the forming quality of a large diaphragm for a television speaker, infrared heating was added to the process to preheat the TPU film before the forming stage. Various processing parameters including ultrasonic thermoforming and infrared heating conditions were investigated in relation to the forming quality. As a consequence, the diaphragm could be fabricated with acceptable forming ratios (> 95 % in the band region and > 70 % in the micro-corrugations) and short cycle time (12 s). This means that the proposed process is superior to conventional thermoforming processes that require long cycle time (> 200 s).

Keywords: Ultrasonic thermoforming; Speaker diaphragm; Micro-corrugation; Infrared heating

1. Introduction

Thermoforming is a process in which a thin polymer film is softened and deformed over a mold into the desired shape by imposing appropriate heating and pressure [1]. In general, the thermoforming process requires long cycle time (Up to several minutes) for appropriate mold temperature control. That is, thermoforming molds should be heated to higher than the softening temperature of polymer film before the forming stage, and should then be cooled below the softening temperature for proper demolding after the forming stage [2].

In the past decade, ultrasonic fabrication technologies have been applied to facilitate traditional polymer processing methods [3]: Injection molding [4-6] and hot embossing [7-9]. In these processes, ultrasonic vibration energy was used as an auxiliary energy source for heating and softening thermoplastic polymer. Ultrasonic imprint lithography was then further applied to direct fabrication of polymer micropatterns without the use of thermal energy [10-12].

Recently, ultrasonic vibration energy has also been applied for thermoforming of thin polymer films [13-15]. In these studies, a micro-speaker diaphragm for a mobile phone speaker was developed by applying ultrasonic thermoforming. A diaphragm (13.8 × 9.8 × 0.47 mm) was formed out of 32 μm Polyetheretherketones (PEEK) film. To prevent damage of such a thin film during ultrasonic vibration, a soft elastomer mold was used instead of a metal mold [14], and the effect of its location (i.e., whether installed above or below the polymer film) was investigated in terms of formability of the diaphragm [15].

This study extends the ultrasonic thermoforming process to the fabrication of a large diaphragm for a television speaker (80.1 × 18.4 × 1.7 mm). This is much larger than that of the previous micro-speaker diaphragm for a mobile phone. An ultrasonic sonotrode was designed and analyzed numerically in order to obtain uniform vibration characteristics. Ultrasonic thermoforming experiments were performed using the optimally designed sonotrode. To improve the forming quality of the large diaphragm, infrared heating was added to the process to preheat the polymer film before the forming stage. Various process parameters, including ultrasonic thermoforming and infrared heating conditions, were then investigated to obtain better forming quality. The forming results were compared with the results from conventional thermoforming in terms of the forming quality and the cycle time of the forming process.

*Corresponding author. Tel.: +82 2 970 6358, Fax.: +82 2 974 8270
E-mail address: kpark@seoultech.ac.kr
This paper was presented at the ICMDT2017, Ramada Plaza Jeju Hotel, Jeju, Korea, April 19-22, 2017. Recommended by Guest Editor Dong-Gyu Ahn.

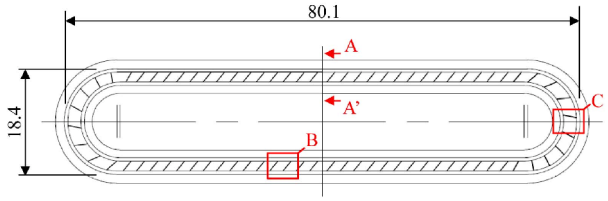

Fig. 1. Configuration of the television speaker diaphragm (Unit: mm).

2. Ultrasonic thermoforming of large film

2.1 Overview of ultrasonic thermoforming

A speaker diaphragm is a key component of a speaker module that generates desired vibration characteristics and sound responses within the audible frequency range. For a micro-speaker module, polymer diaphragms are generally used instead of the conventional pulp diaphragms, owing to their greater flexibility and durability [16]. The polymer diaphragm is formed out of thin polymer films, and is assembled with a voice coil and magnets for proper electromagnetic interaction [17]. Fig. 1 shows the dimensional configuration of the television speaker diaphragm, of which dimensions were 80.1 mm long, 18.4 mm wide, and 270 μm thick. A band with rectangular shape and rounded corners was to be protruded to a depth of 1.5 mm, and a number of micro-corrugations (700 μm wide and 200 μm high) were to be formed on the surface of the protruded band surface. The marked regions (Sec. A-A′, regions B and C) will be referred to in the following sections for discussion of forming quality.

This diaphragm was fabricated using thermoforming process in which a thin Thermoplastic polyurethane (TPU) film was shaped into a part with the desired form. In the thermoforming process, the TPU film was heated above its softening temperature in a heating chamber, and was shaped over a mold under the given pressure conditions [18]. For proper heating, the chamber and mold were heated from the initial temperature (40 °C) to the target temperature (150 °C). After forming, the heated chamber and mold were then cooled for proper removal of the formed film. This process required 160 s cycle time that consisted of 130 s heating time and 30 s cooling time.

To reduce the cycle time, ultrasonic thermoforming was introduced in this study. Fig. 2 illustrates the configuration of the ultrasonic thermoforming system, which consists of an ultrasonic unit, a pressing unit, a control unit, and a forming section. The ultrasonic unit contains an ultrasonic generator and a booster, and generates ultrasonic waves at 19.8 kHz and with power of 1.4 kW. The pressing unit imposes pneumatic pressure during the vibration and holding stages. In the forming section, a TPU film is installed between the mold and a holder. The mold was fabricated in a concave shape of the protruded feature, and two cartridge heaters were inserted for mold heating. An ultrasonic sonotrode was fabricated as a convex shape of the protrued feature, and was installed at the bottom of the ultrasonic unit. Ultrasonic waves were then transferred to the sonotrode, at which the TPU film was softened enough to be formed into the desired shape.

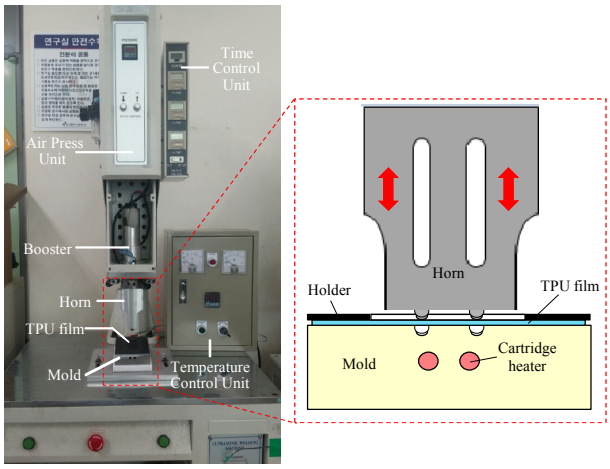

Fig. 2. Configuration of ultrasonic thermoforming system with a detail view of the forming section.

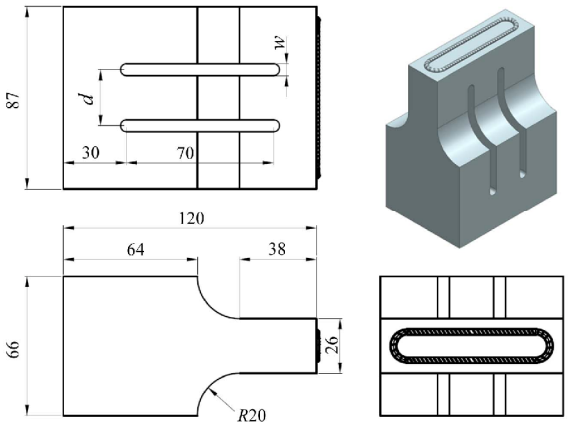

Fig. 3. Dimensional configurations of the sonotrode with vertical slots.

2.2 Design and analysis of an ultrasonic sonotrode

In this study, an ultrasonic sonotrode was designed to include the diaphragm shape on its tip (87 × 26 mm), as shown in Fig. 3. Considering that this sonotrode is much larger and wider than those from previous studies [13-15], its vibration characteristics may not be uniform across the whole outlet section. Two vertical slots were then added to improve the uniformity of the sonotrode vibration and to ensure better forming quality. Two slot design parameters, slot width (w) and distance (d), were considered and evaluated to improve the vibration characteristics.

Finite element (FE) modal analysis was performed to investigate the vibration characteristics of the sonotrode. ANSYS Multiphysics™ (ANSYS Inc., USA) was used in the FE modal analysis. AA7075-T651 was used as the sonotrode material: its density and elastic modulus were 2810 kg/m^3 and 71.7 GPa, respectively.

Figs. 4(a) and (b) show the longitudinal displacement of the

Table 1. Design table with the slot parameters and FE analysis results.

No	w (mm)	d (mm)	f (kHz)	Deviation (%)
1	4.0	40	19.47	10.29
2	6.5	30	19.72	5.75
3	6.5	30	19.72	5.75
4	10	30	19.13	14.80
5	3.0	30	20.23	10.55
6	4.0	20	20.10	11.12
7	9.0	20	19.37	20.96
8	6.5	30	19.72	5.75
9	6.5	44.1	19.75	17.85
10	6.5	30	19.72	5.75
11	9.0	40	19.37	20.95
12	6.5	15.9	19.72	3.98
13	6.5	30	19.72	5.75

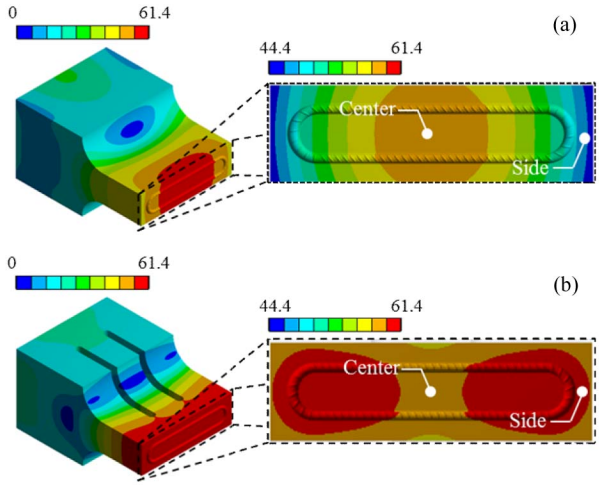

Fig. 4. Comparison of the longitudinal vibration amplitudes: (a) Plain sonotrode; (b) sonotrode with two vertical slots.

plain sonotrode without a slot and the sonotrode with two vertical slots (*w*: 6.5 mm, *d*: 30 mm), respectively. It can be seen that the plain sonotrode shows larger deviation (24.5 %) in its vibration amplitude at the tip, where the amplitude of the central region was higher than those of the side regions. On the other hand, the slotted sonotrode shows much smaller deviation (5.75 %). This indicates that removal of the slot volume has the effect of increasing the vibration of the side regions so that the uniformity in the outlet vibration can be improved.

To investigate the effect of the slot design on the vibration characteristics, a Design of experiment (DOE) was performed using the Central composite design (CCD) table. Thirteen experiments were scheduled as listed in Table 1, with variation of two slot-design parameters (*w* and *d*). Two resulting responses were selected for response surface analysis for optimization: (i) The natural frequency of the sonotrode (*f*) and (ii) the deviation of the sonotrode vibration at its outlet. For

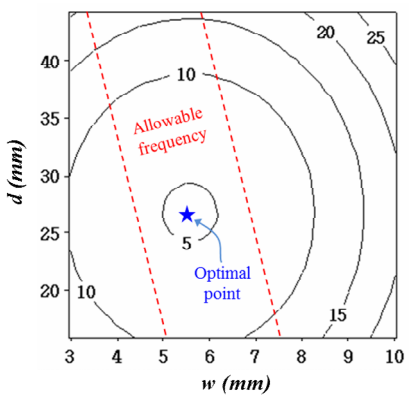

Fig. 5. Response contour for deviation of the vibration amplitude.

Fig. 6. Photographs of the fabricated diaphragm: (a) Top view; (b) sectional view (Sec. A-A′).

the optimization, the target natural frequency was set to the range 19.8 ± 0.15 kHz which is the allowance of the resonance frequency. Optimization was then performed to minimize the deviation based on the resulting response contour within the allowable frequency range (Fig. 5). The optimal slot width (*w*) and distance (*d*) were determined to be 5.6 and 26.7 mm, respectively. Additional FE analysis was performed under optimal conditions, and the resulting deviation was further reduced to 4.75 %. The calculated natural frequency was 19.802 kHz, which is within the allowable range. The ultrasonic sonotrode was then fabricated based on the optimal design.

2.3 Ultrasonic thermoforming experiment

Ultrasonic thermoforming experiments were performed using the fabricated sonotrode. Mold temperature and ultrasonic vibration time were set to 30 °C and 5.0 s, respectively. After ultrasonic vibration was the holding stage, during which the forming section was held under 0.3 MPa pressure for 4.0 s. Fig. 6 shows photographs of the fabricated diaphragm from the top and sectional views. The height of the protruded band was 0.40 mm, which corresponds to a 26.7 % forming ratio, in comparison with the desired dimension (1.5 mm).

To improve the forming ratio, additional experiments were performed with variations in the mold temperature (80, 90, 100 °C) and vibration time (5, 7, 9 s). Figs. 7(a) and (b) compare the forming ratios at different mold temperatures and vibration times. It can be seen that the forming ratios were improved as both conditions increased. However, the highest forming ratios were still around 60 % in both cases: 66.2 % at 100 °C mold temperature and 62.1 % at 9 s vibration time. Moreover, the TPU film stuck to the mold surface when the

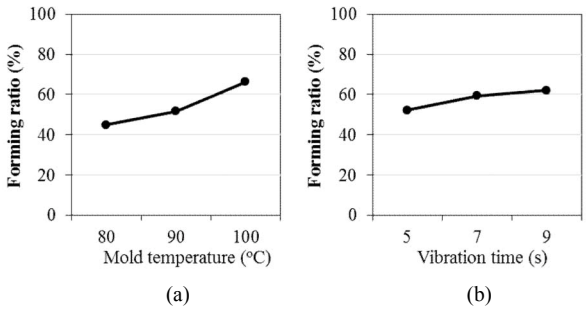

Fig. 7. Changes of forming ratio with variations in forming conditions: (a) Mold temperature; (b) vibration time.

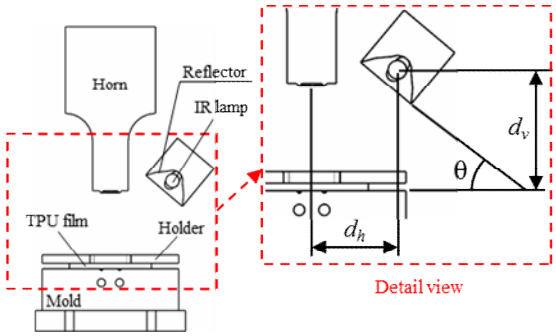

Fig. 8. Schematic description of the infrared heating equipment.

mold temperature was higher than 100 °C. This indicates that additional increase in the mold temperature is not desirable considering proper demolding after thermoforming. Based on these results, it can be concluded that the large TPU diaphragm could not be fabricated by ultrasonic thermoforming only unlike the previous studies [14-15].

3. Ultrasonic thermoforming with infrared heating

3.1 Infrared heating as an auxiliary heat source

To improve the forming ratio of the diaphragm, infrared (IR) heating was applied to preheat the TPU film before the forming stage. Fig. 8 shows a schematic description of the infrared heating equipment. An infrared lamp (850 nm wavelength, 500 W power) was installed above the TPU film and beside the sonotrode. Infrared light was radiated on the upper face of the TPU film, and the sonotrode moved downward for ultrasonic excitation. Thus, the upper surface of the TPU film became heated and its forming quality was improved.

To analyze the irradiation characteristics of the proposed infrared heating equipment, ray tracing simulation was performed using SPEOS (OPTIS, France). Figs. 9(a) and (b) show the ray tracing simulation results and the resulting radiance distribution of the TPU surface. It can be seen that the metal holder acts as a mask, and only the inside region is affected by the infrared radiation. An infrared heating experiment was performed, and the resulting heating capability was measured using a thermal imaging system (FLIR E50, FLIR Systems Inc., France). Fig. 9(c) shows the temperature distribution of the TPU surface after 2 s of irradiation. This shows that the target area could be heated to its softening temperature (150 °C) using IR. The proposed IR heating is advantageous not only for its rapid heating capability but also because it can be used without demolding issues; the TPU film did not stick to the mold or holder after the localized heating.

Table 2. Design table for the infrared illumination conditions.

No	θ(°)	d_h (mm)	d_v (mm)	R_m (W/m^2)	ΔR (W/m^2)
1	32	34	61	37106.6	3271
2	38	34	61	36482.8	1183
3	32	40	61	34449.3	8345
4	38	40	61	33716.2	1314
5	32	37	58	38201.1	5962
6	38	37	58	38105.8	798
7	32	37	64	34242.0	8776
8	38	37	64	34232.3	294
9	35	34	58	39115.4	2189
10	35	40	58	35215.1	7548
11	35	34	64	35593.7	543
12	35	40	64	33097.7	2263
13	35	37	61	35845.4	1728
14	35	37	61	35478.5	1887
15	35	37	61	35871.3	2432

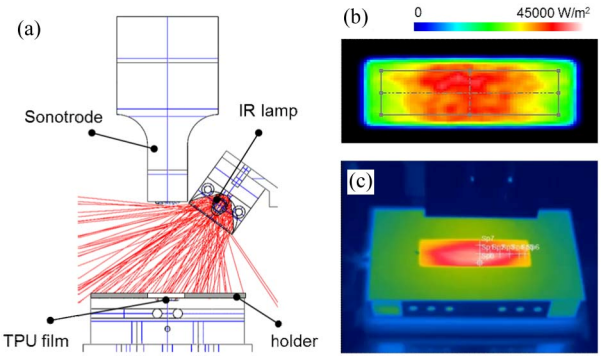

Fig. 9. Optimal simulation results for infrared heating: (a) Ray tracing results; (b) radiance distribution; (c) temperature distribution.

3.2 Optimization of infrared illumination conditions

As illustrated in Fig. 8, the lamp unit was installed to have a certain angle of inclination (θ), as well as horizontal (d_h) and vertical (d_v) distances from the film center. Therefore, infrared rays illuminated the film to varying degrees depending on the inclination; so the radiance on the TPU film was different according to its location. That is, the radiance at the close point (P_1 in Fig. 10) is obviously higher than that at the far point (P_2 in Fig. 10).

To compare the effects of the aforementioned three parameters (θ, d_h and d_v) on the irradiation characteristics, ray tracing simulation was conducted. A DOE was performed using CCD

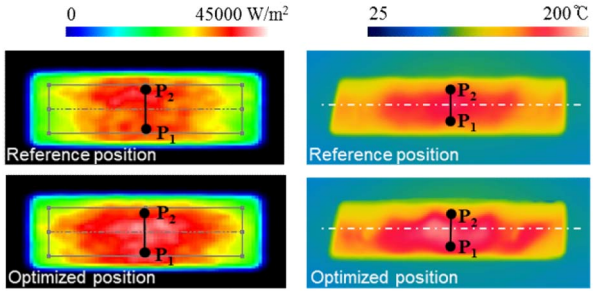

Fig. 10. Comparison of the IR irradiation results for the reference and optimized positions: (a) Radiance distribution (Simulation); (b) temperature distribution (Experiment).

design, and fifteen experiments were scheduled as listed in Table 2. Two responses were selected for response surface analysis for optimization: (i) The mean value of the radiance on the TPU surface (R_m) and (ii) the deviation of radiance between P_1 and P_2 (ΔR).

Through the statistical analysis, regression models of the response surfaces for the mean (R_m) and deviation (ΔR) were obtained as given in Eqs. (1) and (2), which were used as the objective functions for optimization.

$$R_m = 88246.9 - 492.512\, d_h - 561.319\, d_v \quad (1)$$

$$\Delta R = 17496.7 - 948.542\, \theta + 511.833\, d_h . \quad (2)$$

The optimal design parameters were then calculated based on these regression models. The objectives of the optimization were to maximize the mean radiance (R_m) and minimize the radiance deviation (ΔR). The optimal parameters were then determined as follows: $\theta = 36°$, $d_h = 34$ mm and $d_v = 59$ mm. Fig. 10(a) compares the radiance distributions of the reference case ($\theta = 35°$, $d_h = 37$ mm and $d_v = 61$ mm) and the optimized case. The mean radiance under the optimized position was 39109 W/m^2, which corresponds to a 9.02 % increase from that at the reference position (35871 W/m^2). The radiance deviation under the optimal condition was 170 W/m^2, only 6.99 % of the reference case (2432 W/m^2).

IR heating experiments were then performed for the aforementioned reference and optimized positions. In Fig. 10(b), the temperature distributions of the TPU films in the reference and optimized cases are compared, showing that the optimized case showed more uniform temperature distribution than did the reference case. The temperature difference of the reference and optimized case was 5.4 and 1.5 °C, respectively. Therefore, it can be concluded that uniform IR illumination ensured uniform heating of the target polymer surface.

3.3 Ultrasonic thermoforming with infrared heating

Ultrasonic thermoforming experiments were performed with the aid of infrared heating. For ultrasonic thermoforming, the mold temperature and ultrasonic vibration time were set to 80 °C and 4.0 s, respectively. After ultrasonic vibration, the holding stage followed with 0.3 MPa holding pressure for 4.0 s. IR heating was performed from both the reference and optimized positions, for 3.0 s heating time. After thermoforming, the heights of the protruded band and micro-corrugations were measured using an optical microscope (Mi-9000, Jason Electro-Tech, Republic of Korea).

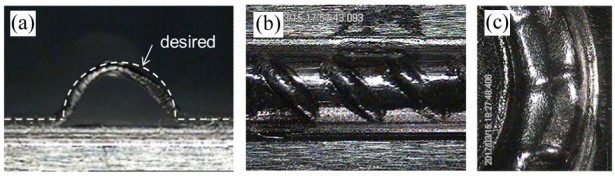

Fig. 11. Photographs of the fabricated diaphragm under infrared heating: (a) Sectional view (Sec. A-A′); (b) straight region (Region B); (c) curved region (Region C).

Figs. 11(a)-(c) show photographs of the fabricated diaphragm under IR heating. Fig. 11(a) shows a sectional view of the Sec. A-A′. It can be seen that the height of the band almost reached to the design dimension. This result is a significant improvement compared with the previous result without IR heating (Fig. 6(b)). Figs. 11(b) and (c) show photographs for the straight (B) and curved (C) regions of the protruded bands with micro-corrugations. The forming ratio for the protruded bands were 98.4 ± 6.10 % for the straight region and 98.3 ± 3.82 % for the curved region. This showed significant improvement in comparison with the previous results without IR heating (Fig. 7). On the other hand, for the micro-corrugations, the forming ratio was 45.4 ± 8.41 % for the straight region and 53.8 ± 4.85 % for the curved region. Therefore, further study was required to improve the forming quality of these micro-corrugations.

3.4 Effect of the ultrasonic thermoforming conditions

In this section, the effects of ultrasonic thermoforming conditions were investigated to further improve the formability of the micro-corrugations. The reference processing conditions for ultrasonic thermoforming were set to be the same as for the previous case in Sec. 3.3. Among these processing conditions, four parameters (Vibration time, holding time, holding pressure, and heating time) were varied separately, and the resulting forming ratios were compared for the corrugation regions.

Figs. 12(a)-(d) show variations of the forming ratio of micro-corrugations according to the variation of each processing condition. It can be seen that the IR heating time was linked to a significant improvement in the forming ratios in both the straight and curved regions, as shown in Fig. 12(d), while the other conditions were not. The infrared heating time was then set to 4 s. Under this condition, the forming ratios were higher than 70 % in both regions.

To this point, the forming ratios had been measured by analyzing optical microscope images of the fabricated diaphragm,

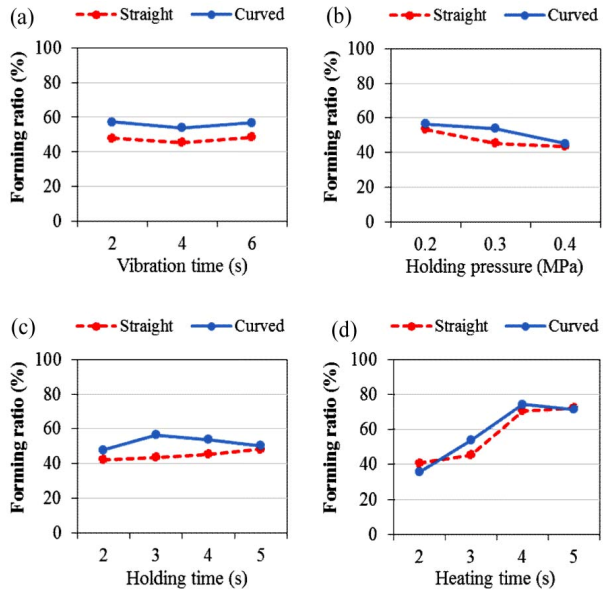

Fig. 12. Comparison of forming ratios at micro-corrugations with variations in various processing conditions: (a) Vibration time; (b) holding pressure; (c) holding time; (d) IR heating time.

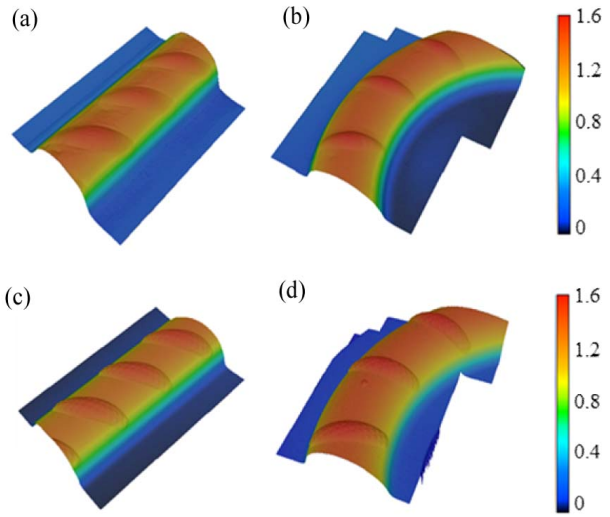

Fig. 13. Measured surface profiles of micro-corrugations: (a) Straight region (Ultrasonic thermoforming); (b) curved region (Ultrasonic thermoforming); (c) straight region (Pure thermoforming); (d) curved region (Pure thermoforming).

such as is Figs. 6(b) and 11(a). These sectional images were obtained after cutting a cross-section through the fabricated diaphragms (A-A′), as marked in Fig. 1. However, this method resulted in a measurement error because the forming height might change after cutting due to elastic recovery.

For more precise measurement of the forming ratios of the micro-corrugations, the surface profiles of the determined processing conditions (i.e., 80 °C mold temperature, 2.0 s vibration time, 0.2 MPa holding pressure, 3.0 holding time and 4.0 s IR heating time) were measured using a laser microscope (VK-X200, Keyence Co., Japan). Figs. 13(a) and (b) show the surface profiles of the diaphragm fabricated by ultrasonic thermoforming. It can be seen that the micro-corrugations were well developed, and the resulting forming ratios were 75.0 % for the straight region (B) and 76.6 % for the curved region (C). Figs. 13(c) and (d) show the surface profiles of a commercially used diaphragm that was fabricated by pure thermoforming. The forming ratios of the micro-corrugations were measured to be 94.3 % for the straight region (B) and 92.2 % for the curved region (C). Thus, the ultrasonically thermoformed sample showed forming quality as much as 80 % of that of the pure thermoformed sample.

4. Conclusions

In this study, ultrasonic thermoforming was implemented for fabrication of a large TPU diaphragm for a television speaker, instead of conventional thermoforming. To fabricate the large diaphragm with allowable dimensional accuracy, the following approaches were used: (i) FE modal analysis was used to optimize the vibration uniformity of the large sonotrode; (ii) IR heating was used to preheat the TPU film without creating a demolding problem; (iii) the IR lamp position was optimized to ensure uniform heating capability; and (iv) the ultrasonic thermoforming conditions were investigated to obtain high forming quality, not only in the protruded band, but also in the micro-corrugations.

As a consequence, the average forming ratio of the protruded band and the micro-corrugations were improved to 98 % and 75 %, which can be regarded as within an acceptable range for speaker quality. The total cycle time of the ultrasonic thermoforming was as short as 9 s including 4 s heating, 2 s vibration, and 3 s holding time. This cycle time corresponds to less than 1/10 that of the conventional thermoforming process (160 s). Moreover, the proposed ultrasonic thermoforming process has the advantage that it can be performed in an open space so that it can be automated for mass production, unlike conventional thermoforming that must be performed in a closed chamber.

Acknowledgment

This study was financially supported by the Commercialization Promotion Agency for R&D Outcomes, Ministry of Science, ICT and Future Planning, Republic of Korea.

Nomenclature

w	: Slot width of the ultrasonic sonotrode
d	: Slot distance of the ultrasonic sonotrode
θ	: Angle of incline of the IR heating equipment
d_h	: Horizontal distance to the IR heating equipment
d_v	: Vertical distance to the IR heating equipment
R_m	: Mean value of the radiance
ΔR^*	: Deviation of the radiance

References

[1] J. L. Throne, *Technology of thermoforming*, Hanser Verlag GmbH & Co, Munich (1996).

[2] H. J. Lee and D. G. Ahn, Manufacture of a large-sized Flat panel airlift Photobioreactor (FPA PBR) case, *J. Mech. Sci. Technol.*, 29 (12) (2015) 5099-5105.

[3] J. Sackmann, K. Burlage, C. Gerhardy, B. Memering, S. Liao and W. K. Schomburg, Review on ultrasonic fabrication of polymer micro devices, *Ultrasonics*, 56 (2015) 189-200.

[4] A. Sato, H. Ito and K. Koyama, Study of application of ultrasonic wave to injection molding, *Polym. Eng. Sci*., 49 (4) (2009) 768-773.

[5] W. Michaeli, T. Kamps and C. Hopmann, Manufacturing of polymer micro parts by ultrasonic plasticization and direct injection, *Microsyst. Technol*., 17 (2) (2011) 243-249.

[6] M. Sacristana, X. Plantaa, M. Morellc and J. Puiggalic, Effects of ultrasonic vibration on the micro-molding processing of polylactide, *Ultrason. Sonochem*., 21 (1) (2014) 376-386.

[7] H. Mekaru, H. Goto and M. Takahashi, Development of ultrasonic micro hot embossing technology, *Microelectron Engng.*, 84 (5-8) (2007) 1282-1287.

[8] W. K. Schomburg, K. Burlage and C. Gerhard., Ultrasonic hot embossing, *Micromachines*, 2 (2) (2011) 157-166.

[9] C. Y. Chang and C. H. Yu, A basic experimental study of ultrasonic assisted hot embossing process for rapid fabrication of microlens arrays, *J. Micromech. Microeng*., 25 (2) (2015) 025010.

[10] H. Mekaru and M. Takahashi, Ultrasonic nanoimprint on poly (Ethylene terephthalate) at room temperature, *Jap. J. Appl. Phys*., 47 (6) (2008) 5178-5184.

[11] W. Jung, H. J. Lee and K. Park, Investigation of localized heating characteristics in selective ultrasonic imprinting, *Int. J. Precis. Engng. Manuf.*, 16 (9) (2015) 1999-2004.

[12] H. J. Lee and K. Park, Variable wettability control of a polymer surface by selective ultrasonic imprinting and hydrophobic coating, *Colloid Polym. Sci.,* 294 (9) (2016) 1413-1423.

[13] H. Bae and K. Park, Design and analysis of ultrasonic horn for polymer sheet forming, *Int. J. Precis. Eng. Manuf. Green Technol.*, 3 (1) (2016) 49-54.

[14] H. Bae, H. J. Lee and K. Park, Ultrasonic assisted thermoforming for rapid fabrication of a microspeaker diaphragm, *Microsyst. Technol*., 23 (6) (2017) 1677-1686.

[15] H. Bae, H. J. Lee and K. Park, Effect of vibration transmission direction in ultrasonic thermoforming on the formability of micro-corrugations, *Int. J. Precis. Eng. Manuf.*, 18 (5) (2016) 697-703.

[16] J. O. Sun and K. J. Kim, Isolation of vibrations due to speakers in audio-visual electronic devices without deteriorating vibration of speaker cone, *J. Mech. Sci. Technol.,* 26 (3) (2012) 723-730.

[17] D. C. Kim and H. Y. Jeong, An optimal design of the internal space in a micro-speaker module. *Int. J. Precis. Eng. Manuf.*, 16 (6) (2015) 1141-1147.

[18] K. M. Kim and K. Park, Numerical investigation on vibration characteristics of a micro-speaker diaphragm considering thermoforming effects, *J. Mech. Sci. Technol.*, 27 (10) (2013) 2923-2928.

[19] W. Liang, Y. Liu, B. Zhu, M. Zhou and Y. Zhang, Conduction heating of boron alloyed steel in application for hot stamping. *Int. J. Precis. Eng. Manuf.*, 16 (9) (2015) 1983-1992.

Hyun-Joong Lee is a Ph.D. candidate in the Department of Mechanical Design and Robot Engineering at Seoul National University of Science and Technology, Korea. He received his B.S. and M.S. degrees from Seoul National University of Science and Technology, in 2013 and 2015, respectively. His current research includes ultrasonic fabrications of polymer parts including ultrasonic imprinting and ultrasonic thermoforming processes.

Keun Park received his B.S. and M.S. degrees in Precision Engineering and Mechatronics from KAIST, Korea, in 1992 and 1994, respectively. He then received his Ph.D. degree in Mechanical Engineering from KAIST in 1999. Dr. Park is currently a Professor of the Department of Mechanical System Design Engineering at Seoul National University of Science and Technology, Korea. His research interests include numerical analysis of material forming processes, micro-fabrication, and additive manufacturing.